Graphene-based nano-rectenna in the far infrared frequency band

Diego Masotti, Alessandra Costanzo, Marco Fantuzzi, Franco Mastri
DEI
University of Bologna
Bologna, Italy
diego.masotti@unibo.it

Martino Aldrigo, Mircea Dragoman
MIMOMEMS
IMT
Bucharest, Romania
{martino.aldrigo;mircea.dragoman}@imt.ro

***Abstract*—In this paper we propose a realistic nano-rectenna able to harvest from human heat in the infrared frequency band (around 30 THz). The full-wave designs of both an array and a multi-element antenna are presented, taking into account the non-trivial behavior of gold at these frequencies. The use of an original diode realized on a graphene layer, and the derivation of its model from ballistic theory, allow to compare the rectifying performance from both modelling and measurements point of view. Encouraging results in terms of both rectified current of a single nano-rectenna and of power rectified by a macro-system combining thousands of nano-rectennas are shown.**

Keywords— Energy-harvesting; printed antenna; antenna array; infrared region; graphene diode

I. INTRODUCTION

The need for wireless communication and sensing capabilities in ambient-embedded micro-systems is increased in the last years, and this has stressed the importance to reach energy autonomy for these distributed devices. Among them, ultra-low power microcontrollers and sensors require small amounts of power (ranging from a few μW to a few hundreds of μW) few times per day. As a consequence the exploitation of ambient energy sources is a key point in emerging green technologies.

The collection of energy from environmental RF sources is a potential solution to this problem, as demonstrated in [1,2]. However the available amount of RF energy is low, even in highly humanized environments [3] and typically only few μW of power can be provided by highly efficient rectennas. To face the lack of power technological improvements must be adopted by RF harvesters: power management units based on switching converters for efficiently biasing the rectenna [4,5] or new rectifying section topologies [6].

More than 40% of the total energy radiated by the sun covers the infrared (IR) region (up to 400 THz). In this frequency region the available power amount is greater than in RF range and research activities in the field of nano-rectennas in the THz spectrum start to arise [7,8]. Strong limitations arise from the nature of the materials at THz frequencies, especially from conductor losses [9]. However the undisputed bottleneck in THz rectenna realization is the lack of rectifying diodes at this frequency range. The widely diffused tunnel Metal-Oxide-Metal diode [10] has shown its poor rectification properties in THz-DC conversion [8].

In this paper we try to bridge the gap by introducing the first diode on graphene able to rectify IR power up to 30 THz. The diode has been realized and measured in the IMT Lab, Bucharest, Romania. Due to the actual diode frequency limit we imagine to harvest energy from human heat (the energy peak being around 31 THz). The corresponding optimized nano-rectenna, exploiting traditional materials, is then rigorously characterized from the nonlinear and electromagnetic (EM) point of view, by resorting to: (i) the full-wave description of the array; (ii) the EM theory for the rigorous prediction of available THz power in the nano-antenna location; (iii) the measured graphene diode I-V characteristics. Encouraging rectified current levels are obtained, thus foreseeing the potential use of the macro-system combining thousands of our nano-rectenna in Body Area Network applications.

In authors' opinion the extension of the frequency range of diode rectifying capabilities can be obtained by a further miniaturization of the device itself. This will probably lead to the realization of THz rectennas able to exploit sun radiation and to compete with common solar panels, but with size-reduced and cheaper solutions.

II. NUMERICAL APPROACH DESCRIPTION

One of the most challenging problems in harvester optimization is the accurate evaluation of the available power in the antenna location. In the present application, we imagine to harvest from human heat at 31 THz: therefore we focus our investigations in the band [24 – 36] THz in order to evaluate the incident power extracted from the human body, by integrating Planck's law:

$$\frac{dI}{d\lambda} = 2\pi c \frac{1}{\lambda^5} \frac{hc}{\exp\left(hc \Big/ \lambda K_B T\right) - 1} \qquad (1)$$

where I is the spectral irradiance, h is the Planck's constant, c is the light speed (in vacuum), K_B is the Boltzmann's constant and T is the temperature.

Due to the adopted frequency range the nano-rectenna and the THz source can be considered in the far-field region, even in the conceived situation of a worn harvesting system (as will be discussed in Section V). Taken this for granted, we resort to the EM theory [5] for the evaluation of the Norton current generator $J_{human,eq}$, equivalent to the incoming field, according to the schematic picture reported in Fig. 1, where $Y_A(\omega)$ is the full-wave description of the receiving nano-antenna proposed in Section III.

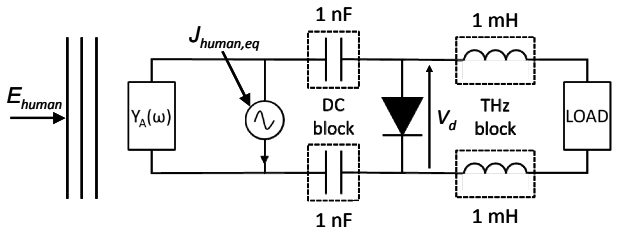

Fig. 1. Equivalent circuit of the THz rectenna.

The straightforward computation of Eq. (1) provides a realistic value of 152.593 W/m^2 of incident power density in the band of interest.

This way a circuit simulation based on the Harmonic-Balance technique can be easily carried out.

III. Base Antenna and Array Design by Full-Wave Numerical Simulation

In RF energy harvesting applications different rectenna architectures can be deployed, depending on the actual scenario under exam: (i) a single antenna-single rectifier solution is generally preferable in ultra-low power situations when the direction of arrival (DOA) of the source is unknown: the antenna works at its best conditions and the diode losses are minima; (ii) a single array-single rectifier solution is more suitable in known DOA of the signal, maintaining diode losses at their minimum; (iii) a multi antenna-multi rectifier solution, where the array-factor is lost, thus better for unknown DOA: here the EM coupling between antennas must be taken into account and the diodes can add more losses with respect to other choices.

For the new THz application under exam we have decided to compare the architectures (ii) and (iii), since the solution (i) is in some way contained in (iii) and, most of all, it would request a huge number of diodes.

A. Planar misaligned bow-tie antenna

As base-antenna on a SiO_2 substrate support we resort to a planar bow-tie antenna, preferable to the simple dipole antenna for a twofold reason: (i) a slightly wider operating bandwidth; (ii) a higher input impedance, suitable to be matched to the loading diode.

From a technological point of view a useful advantage can be taken from a misaligned planar bow-tie topology [7], since no significant variations in the radiating properties derives from misaligning the two antenna monopoles. This choice is mainly due losses considerations in the final array architecture: a gold corporate feed network with two balanced line on the opposite faces of the SiO_2 substrate has proven to be the best choice, with respect to microstrip and coplanar waveguide alternatives. Moreover, a misaligned solution allows to create a more compact array since the monopoles of two neighboring antennas on the opposite side of the substrate can be placed nearer to each other. The graphene diode deposited on the SiO_2 substrate will reach the antenna/array contact on the opposite side by means of a via hole.

The SiO_2 substrate is 300 nm-thick with $\varepsilon_r = 3.9$ e $\tan\delta = 0.001$ @ 31 THz: with thinner solutions no resonance can be detected in the band of interest. The gold metallization is 200 nm-thick, while the total length of the bow-tie antenna is 6.8 μm (including a gap between the two misaligned monopoles for feeding purposes): each monopole is 4.24 μm-long, with an aperture angle of 60°.

For previous considerations, the description of gold losses is particularly delicate in the present design. The surface impedance of the gold has been accurately characterized in the EM simulator [11]. In Fig. 2 the behavior of this quantity is reported within the frequency band of interest.

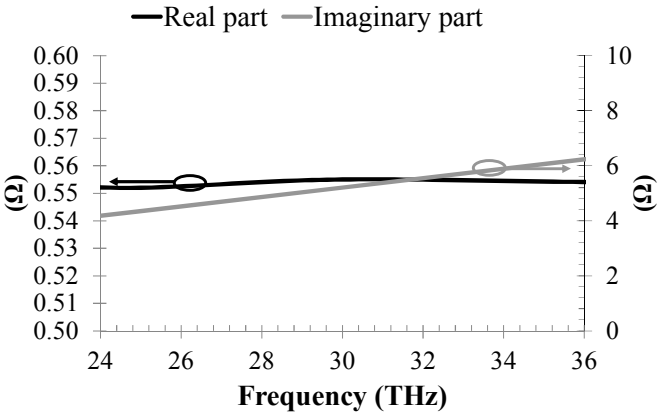

Fig. 2. Simulated surface impedance of gold in the [24 - 36] THz band.

This information allows to evaluate the surface impedance power loss due to gold: for the present bow-tie antenna this loss is equal to 3.8 dB.

B. Planar array

As in [7], a preliminary research on the array topology providing a sufficient directivity in a limited space is performed. An optimization of the radiating properties, taking into account the actual radiation diagram of the base antenna, is carried out by using the number of rows, the number of columns and the distance between the elements as design parameters. The selected topology results to be a 4x2 array with 0.8 λ element spacing (at 31 THz).

A delicate issue is the design of the feeding network. As previously assessed we resort to a balanced line with a characteristic impedance of 98.5 Ω. λ/4 transformers are used at each junction for matching purposes.

In spite of the number of elements the total array efficiency is acceptable: a simulated value of 53% is obtained at 31 THz. In the broadside direction ($\theta = 0°$) the array provides a directivity of 23.66 (13.74 dBi). Fig. 3 shows the array topology with the superposition of the broadside radiation surface. The impedance of the one-port array is given in Fig. 4 in the whole bandwidth: the almost resonant behavior at the desired central frequency is evident from figure inspection. The antenna impedance at 31 THz is about 130 Ω.

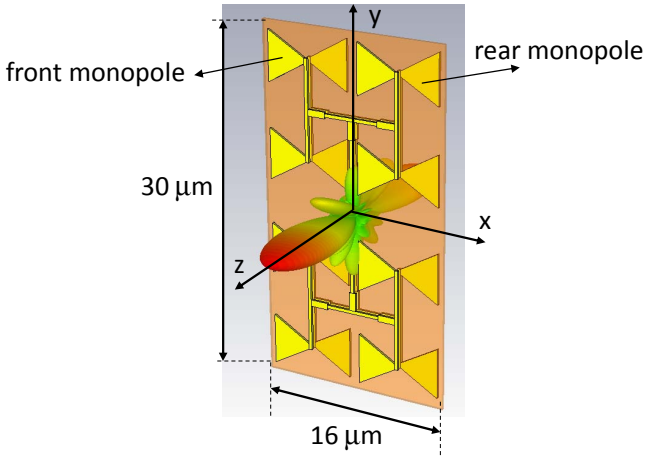

Fig. 3. Array layout with superimposed field radiation surface (linear scale).

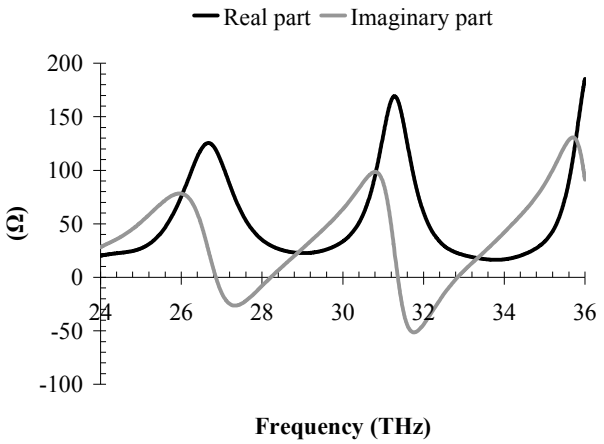

Fig. 4. Simulated array impedance as a function of frequency.

The multi-antenna solution used for comparison has the same area of the array of Fig. 3: 8 separate bow-tie antennas without corporate feed are placed in the same position as in the array configuration. In this case 8 diodes are positioned at each balanced port. The drawback of this solution is that the array factor is lost and that the radiation pattern of each antenna in presence of the remaining 7 parasitic elements has to be considered in the 8 equivalent Norton generators evaluation. The advantage is the absence of the corporate feed, and thus a radiation efficiency for each element of about 98%.

IV. Graphene Ballistic Diode

The major novelty of this paper consists in the exploitation of a graphene ballistic diode for THz rectification, recently presented in [12]. It works up to about 30 THz. According to the Ballistic Theory, no reflections occur within the graphene used as a conductor between two contacts. At room temperature, the ballistic transport in graphene occurs for a mean-free path L_m of 0.4 µm (L_m is distance that an electron travels until its initial momentum is destroyed), reaching an intrinsic mobility of 44,000 $cm^2 \cdot V^{-1} \cdot s^{-1}$.

The theoretical I-V dependence of the graphene diode was calculated using the Landauer formula

$$I(V) = G_q \cdot M \cdot T(V) \cdot V \tag{2}$$

$$G_q = \frac{2e^2}{h} = \frac{1}{12.9\,[k\Omega]} \tag{3}$$

$$M = Int\left[\frac{k_F W}{\pi}\right] \tag{4}$$

where G_q is the quantum unit of the quantized conductance, M is the number of transverse modes propagating in the diode, W is the graphene conductor width, k_F is the Fermi wavenumber, and $T(V)$ is the voltage-dependent transmission coefficient in the graphene layer. Eq. (2) was found by dividing the total area of the diode in a certain number of regions, solving the Dirac equation in each region and imposing the continuity conditions at each interface for the spinorial solutions of the Dirac equation. It was found that the diode has a certain region where the current is nearly zero of width $\pi\hbar v_F/d_{out}$, with v_F the Fermi velocity in graphene, $\hbar$ the reduced Planck constant, d_{out} output graphene layer dimension. So, the diode exhibits rectifying capabilities in this region and its I-V characteristic is strongly dependent on the Fermi energy, which can be tuned by a gate voltage (V_g). Of course, for harvesting purposes, it must be employed under unbiased condition ($V_g = 0$ V).

The geometric diode was fabricated in the laboratories of IMT on a graphene monolayer wafer deposited by Chemical Vapour Deposition (CVD) on a 4 inch-wafer of 300 nm-thick SiO_2 grown on a 500 µm-thick *p*-doped silicon layer. Fig. 5a shows a schematic of the realized graphene diode with a length L of 100 nm, a shoulder of d_{in} = 100 nm and a neck of only d_{out} = 30 nm, whereas in Fig. 5b a SEM photo of the same diode is depicted.

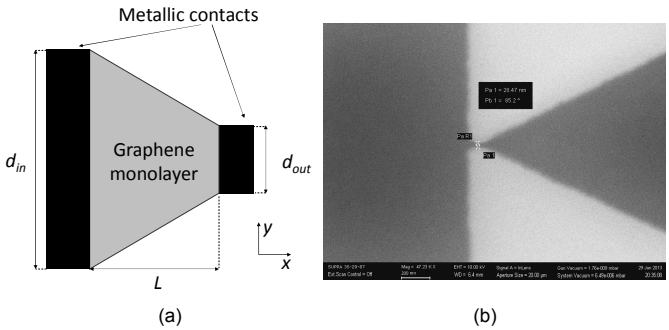

Fig. 5. a) Scheme of the graphene ballistic diode; b) SEM photo of the graphene diode.

The corresponding measured I-V characteristic of the unbiased diode is reported in Fig. 6. It has to be stressed that the measured values of the I-V characteristic provide a leakage current of about 88 pA in correspondence of a voltage of 0 V: this current is due to the high resolution of the measurement set-up and represents the realistic physical operating conditions of the graphene diode. In the subsequent nonlinear simulations this leakage current will be taken into account for the proper modeling of the entire nano-rectenna.

A region of about 140 mV around 0 V exists where the current is very small.

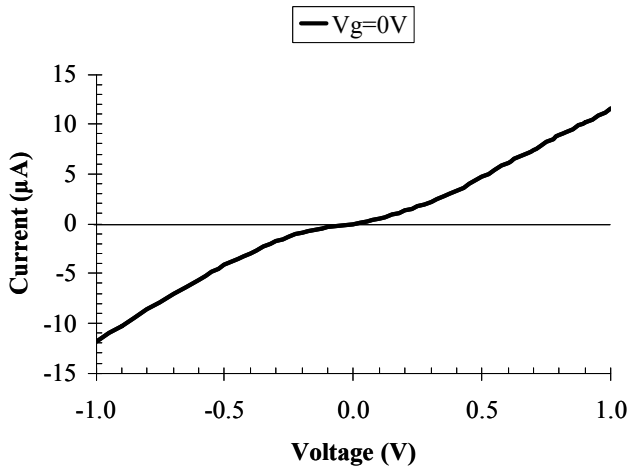

Fig. 6. Measured I-V characteristic of the realized diode.

V. NONLINEAR/EM CO-SIMULATION RESULTS

From the 152.6 W/m^2 of incident power in the band of interest and from the application of the reciprocity theorem [1, 5] we quantify the equivalent Norton generator ($J_{human,eq}$ of Fig. 1) as 24.57 μA at 31 THz. The nonlinear simulation is carried out in a twofold way: by exploiting both the diode model described by (2)-(4) and the measured I-V characteristic of Fig. 6. The results agreement is excellent. This evaluation is carried out at each frequency of the band, by considering the dispersive behavior of the array. According to [13], Fig. 7 displays the rectified DC current I_{DC} on the optimum load of the array (about 160 kΩ, in this case). The DC current was computed to be around 46 pA at 31 THz, whereas the multi-antenna solution exhibits a I_{DC} of about 45 pA at the same frequency. It has to be stressed that no matching circuit has been considered between the bow-tie antenna array and the diode to maximize the power transfer to the rectifier. The number of arrays/multi-antenna that can be placed in 1 cm^2 is equal to 96,516: the array macro-system provides a total DC power of about 33 pW, whereas the multi-antenna macro-system gives a total P_{DC} of about 250 pW.

These results represent a first step towards graphene-based nano-rectennas harvesting applications from infrared energy. The future extension of the cut-off frequency of the diode into the 100 THz region, and possibly a further improvement of its rectifying properties, will allow a direct comparison with the MOM diode performance harvesting from solar energy.

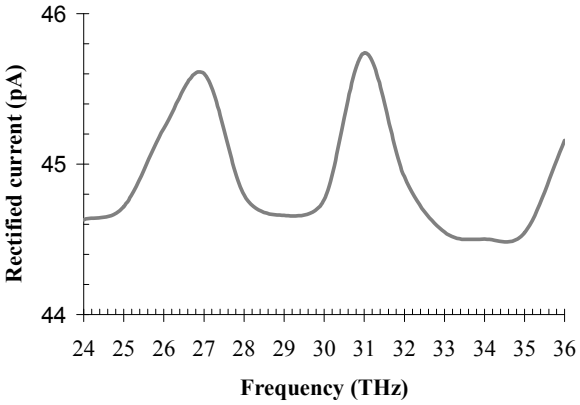

Fig. 7. Simulated rectified current as a function of frequency for the array with a zero-bias graphene diode and a perpendicular incidence of THz radiation.

REFERENCES

[1] D. Masotti, A. Costanzo, M. Del Prete, V. Rizzoli, "A Genetic-Based Design of a Tetra-Band High-Efficiency RF Energy Harvesting System", IET Microwaves Antennas & Propagation, Vol. 7, no. 15, 2013, pp. 1254 – 1263.

[2] J.A. Hagerty, F.B. Helmbrecht, W.H. McCalpin, R. Zane, Z.B. Popovic,"Recycling ambient microwave energy with broad-band rectenna arrays", IEEE Trans. MTT., Vol. 52 , No. 3, 2004, pp. 1014 – 1024.

[3] M. Pinuela, D.C. Yates, P.D. Mitcheson, S. Lucyszyn, "London RF survey for radiative ambient RF energy harvesters and efficient DC-load inductive power transfer," 7th European Conference on Antennas and Propagation (EuCAP), 2013, pp . 2839 - 2843.

[4] A. Dolgov, R. Zane, Z. Popovic, "Power Management System for Online Low Power RF Energy Harvesting Optimization," IEEE Trans. on Circuits and Systems I: Regular Papers, vol. 7, no. 7, pp. 1802-1811, July 2010.

[5] A. Costanzo, A. Romani, D. Masotti, N. Arbizzani, and V. Rizzoli, "RF/baseband co-design of switching receivers for multiband microwave energy harvesting," Sensors and Actuators A: Physical, vol. 179, pp. 158-168, Jun. 2012.

[6] D. Masotti, A. Costanzo, P. Francia, M. Filippi, A. Romani, "A Load-modulated Rectifier for RF Micropower Harvesting with Start-up Strategies," accepted for publication on IEEE Trans. MTT, Feb. 2014.

[7] M. Aldrigo, D. Masotti, V. Rizzoli, A. Costanzo, "Design rules for innovative nano-rectennas in the infrared region," Proc. of 43rd European Microwave Conference (EuMC), Oct. 2013, pp. 1-4.

[8] M. Bareiβ, *et al.*, "Energy Harvesting using Nano Antenna Array", Proc. of the 11th IEEE Int. Conf. on Nanotech. 2011, pp. 218-221.

[9] Ma Zhongkun, G.A.E. Vandenbosch, "Input impedance of optical metallic nano dipole over 300 nm – 1200 nm wavelength," 7th European Conference on Antennas and Propagation (EuCAP), 2013, pp. 3810 – 3813.

[10] A. Sanchez, C. F. Davis, K. C. Liu, A. Javan, "The MOM tunneling diode: theoretical estimate of its performance at microwave and infrared frequencies", J. Appl. Phys., Oct. 1978, vol. 49, No. 10, pp. 5270-5277.

[11] CST Microwave Studio 2013, www.cst.com.

[12] M. Dragoman, M. Aldrigo, A. Dinescu, D. Dragoman and A. Costanzo, "Towards a terahertz direct receiver based on graphene up to 10 THz," J. Appl. Phys., Vol. 115, p. 044307, 2014.

[13] Zixu Zhu, Saumil Joshi, Sachit Grover and Garret Moddel, "Graphene geometric diodes for terahertz Rectennas," J. Phys. D., 2013, vol. 46, pp. 185101-185106.